Journal of Aerosol Science 76 (2014) 126–137

Contents lists available at ScienceDirect

Journal of Aerosol Science

journal homepage: www.elsevier.com/locate/jaerosci

Photophoresis on polydisperse basalt microparticles under microgravity

Markus Küpper [a,*], Caroline de Beule [a], Gerhard Wurm [a], Lorin S. Matthews [b], Jesse B. Kimery [b], Truell W. Hyde [b]

[a] Fakultät für Physik, Universität Duisburg-Essen, Lotharstr. 1, 47048 Duisburg, Germany
[b] CASPER, Department of Physics, Baylor University, One Bear Place 97316, Waco, TX 76798-7316, United States

ARTICLE INFO

Article history:
Received 29 April 2014
Received in revised form
20 June 2014
Accepted 20 June 2014
Available online 30 June 2014

Keywords:
Photophoresis
Planetary atmospheres
Drop tower experiments
Numerical simulations
ΔT−photophoresis
$\Delta\alpha$−photophoresis

ABSTRACT

Photophoresis is a force which can dominate the motion of illuminated aerosols in low pressure environments of laboratory experiments, planetary atmospheres or protoplanetary disks. In drop tower experiments we quantified the photophoretic force on a sample of micrometer-sized basalt grains and aggregates thereof. The particle motions are systematic (linear, helical, in one direction), with most particles moving along the direction of light. Our results are consistent with analytical estimates and numerical simulations of photophoretic forces for small dust aggregates. It implies that the forces are dominated by ΔT−photophoresis with little evidence for $\Delta\alpha$−photophoresis in the micrometer size range.
© 2014 Published by Elsevier Ltd.

1. Introduction

Over the last several decades, photophoretic forces on aerosols have been studied with respect to applications in the middle and the upper atmosphere (Beresnev et al., 2003; Cheremisin et al., 2005, 2011; Hidy & Brock, 1967; Pueschel et al., 2000; Rohatschek, 1956; Wurm & Krauss, 2008). For mesospheric or stratospheric aerosols, photophoresis can be stronger than Earth's gravity and lift particles upwards, possibly acting to concentrate them in certain layers (Beresnev et al., 2003; Cheremisin et al., 2011).

Photophoresis occurs when particles are illuminated by visible or infrared radiation and the resulting surface temperature differs from the surrounding gas temperature. Efficient momentum transfer can occur between the gas and the particle, subjecting the particle to a net force. The effect is strongly pressure dependent and is maximized if the mean free path of the gas molecules, λ, is comparable to the particle size, d, or Knudsen number Kn = 1, where

$$\mathrm{Kn} = \frac{\lambda}{d}. \tag{1}$$

Two extremes of photophoretic forces are discussed in the literature: $\Delta\alpha$ and ΔT forces (Cheremisin et al., 2005).

$\Delta\alpha$ refers to differences in the thermal accommodation coefficient α along a particle surface. The accommodation coefficient quantifies the fraction of gas molecules which are diffusely reflected from a particle surface. Upon re-emission

* Corresponding author.
E-mail address: markus.kuepper.86@uni-due.de (M. Küpper).

http://dx.doi.org/10.1016/j.jaerosci.2014.06.008
0021-8502/© 2014 Published by Elsevier Ltd.

from the surface this fraction of gas molecules takes a momentum determined by the local surface temperature of the particle. The remaining fraction of molecules is reflected specularly with no change in the absolute value of momentum. The accommodation coefficient likely changes over a particle surface, one extreme example being two half spheres with two values of α. In this case a $\Delta\alpha$ force results when the particle has a temperature different from that of the gas as a simple momentum balance implies. As this force only depends on the fact that the particle temperature is different from the gas temperature and as the αs are fixed to the particle, the induced motion is not related to the direction of illumination. $\Delta\alpha$ photophoresis can be viewed as an engine which is fixed to the particle and has a direction only depending on the orientation of the particle. Without alignment, a sample of random particles would set off moving in random directions upon illumination. Small micron sized particles would move on chaotic orbits due to Brownian rotation leading to constant reorientation.

$\Delta\alpha$ photophoresis can be aligned to a certain direction if the particle has a preferred orientation. This is possible in combination with other forces (or torques), such as gravity and gas drag or magnetic torques. If such alignment directs the $\Delta\alpha$ engine upwards and if the photophoretic force is greater in magnitude than gravity, an upward motion can result which has been termed gravitophotophoresis (Cheremisin et al., 2005; Rohatschek, 1996; Rohatschek & Horvath, 2010).

The strength of $\Delta\alpha$ photophoresis is given by (Cheremisin et al., 2005)

$$F_{f\alpha} = \frac{pS\Delta T_S}{4T_\infty}\Delta\alpha \mathbf{e}_{f\alpha}, \tag{2}$$

with p being the gas pressure, T_∞ the undisturbed gas temperature far from the particle, $\Delta T_S = \overline{T} - T_\infty$ the temperature difference between the particle mean temperature $\overline{T}$ and the gas, S the particle surface area and $\mathbf{e}_{f\alpha}$ the unit vector in the direction of the force. $\Delta\alpha$ is calculated as

$$\Delta\alpha = \frac{1}{S}\left|\int_S \alpha \, \mathrm{dS}\right|. \tag{3}$$

Upward motion of particles illuminated from the side has been observed in laboratory experiments (Rohatschek, 1956). As the direction of illumination is different from the direction of lift, it is tempting to assume that $\Delta\alpha$ forces have to act in general on gravitationally aligned particles to explain lifting forces in planetary atmospheres.

However, it is an open question if ΔT forces could not provide a "lift" perpendicular to the direction of illumination as well. In this extreme, the accommodation coefficient is considered to be constant over the particle surface. $\Delta T-$forces relate to photophoresis based on temperature *gradients* along the particle surface. The temperature difference leads to a difference in momentum transferred to accommodated gas molecules. Usually, a particle which is illuminated is heated on the illuminated side; this force is then related to the direction of illumination. The strength of $\Delta T-$photophoresis for a spherical grain is (Rohatschek, 1995)

$$F_{fT} = \frac{1}{2}D\sqrt{\frac{\overline{\alpha}}{2}}r\Delta T_P \frac{2}{\frac{p}{p_{opt}} + \frac{p_{opt}}{p}}, \tag{4}$$

with $\overline{\alpha}$ being the mean accommodation coefficient, ΔT_P the maximum temperature difference over the particle, and $p_{opt} = \sqrt{(2/\overline{\alpha})}(3/\pi)D(T_\infty/r)$. D is a constant determined by the state of the gas defined as a function of the thermal creep coefficient $\kappa = 1.14$, the dynamic viscosity η and the mean thermal velocity v_g

$$D = \frac{\pi}{2}\sqrt{\frac{\pi}{3}}\kappa\frac{v_g\eta}{T_\infty}. \tag{5}$$

For non-spherical, non-homogeneous particles $\Delta T-$forces are not necessarily perfectly aligned to the direction of illumination, but depend on the way the radiation heats the particle. For mm-particles Loesche et al. (2013) showed that the force can be misaligned by several degrees due to shape and compositional effects. If particles in some cases are heated at the back side negative photophoresis is even possible, where particles seem to be attracted by the light source. The situation is more complex if aggregates of particles are concerned, as gas molecules may have a complex collisional behaviour within the boundaries of the aggregate.

One way to shed light on the different potential photophoretic behaviours of natural particles is to carry out experiments under microgravity, where gravity plays no role in alignment and where slow, convection free motions can be measured. This has e.g. been carried out by Wurm et al. (2010), von Borstel & Blum (2012) or Watanabe et al. (2011). The sample in Wurm et al. (2010) consisted of mm sized particles whereas we focus on aggregates here. Watanabe et al. (2011) used smoke particles which essentially all exhibit negative photophoresis and so their focus was on the linearity of the force with illuminating flux. No detailed description of the extreme of negative photophoresis was given. von Borstel & Blum (2012) used aggregates of spherical or irregular micrometer sized particles with aggregate sizes up to 200 μm. This is strongly related to the work presented here but no quantification for the direction of the photophoretic force was presented though these details are likely present in their data. $\Delta\alpha$ forces were also not discussed.

Remaining unknowns are how aggregation changes the direction and strength of the photophoretic force. Particles of a different mineral composition are also of importance. The goal of this work is to quantify photophoretic forces on micrometer basalt particles and aggregates under microgravity. In contrast to the earlier work, these experiments focus on

determining the direction of the force with respect to illumination, as this might be a key to distinguish between $\Delta\alpha$ and ΔT forces. We further present a numerical model to explain the observed variations.

2. Drop tower experiments

A sketch of the experimental setup is shown in Fig. 1. A vacuum chamber is placed in a drop tower capsule providing 9 s of microgravity with a residual gravity below 10^{-6} g at the drop tower in Bremen. A dust bed is placed within the vacuum chamber consisting of basalt with grain sizes below 125 μm. The pressure is preset to a value of 4(± 0.5) mbar. During launch and the final phase of microgravity the sample is covered by a lid to prevent particle loss while the capsule is accelerated and decelerated. 500 ms after onset of microgravity the lid is opened and the dust bed is illuminated by an infrared laser (955 nm) with 20 (± 1) kW/m^2 and a spot diameter of 3.4 cm. The light flux is chosen to allow a combination of different low pressure phenomena (photophoresis, Knudsen compressor, and thermal creep gas flow) to eject particles from the dust bed (de Beule et al., 2013, 2014; Kelling & Wurm, 2009; Wurm & Krauss, 2006). The directed near-infrared radiation enters the dust bed and is absorbed down to a certain depth, heating the top layers. Some heat is conducted downwards, but in addition, the surface can cool by thermal radiation. Therefore, the temperature gradient within the top dust layers differs from the gradient below which generates overpressures and particle ejections (de Beule et al., 2013; Kocifaj et al., 2011).

The collection of data begins when the lid is closed 1 s before the capsule is decelerated. No more dust particles are ejected and a cloud of particles is distributed throughout the chamber (Fig. 2). The airborne particles within the laser beam are subject to photophoretic forces undisturbed by gravity or particle eruptions. The trajectories of the particles within the laser beam are observed with a camera and tracked manually.

2.1. Dust sample

To place photophoretic forces in perspective to our earlier work on light–dust interactions we use the same natural polydisperse basalt sample here. Work on aggregates of monodisperse samples as e.g. used in ground based experiments by Haisch et al. (2008) are also necessary but are only planned for the future. The basalt powder used is commercially available (Kremer Pigmente). No further chemical analysis has been carried out on the sample. The powder is grey in the visual. The sample was sieved before the experiments to obtain only particles smaller than 125 μm. From ground based experiments by Kelling et al. (2011b) it is known that basalt dust sample ejecta have a size distribution as shown in Fig. 3. We assume that the particle size distribution in the experiment is comparable to the measured size distribution function, with an analytical fit given by

$$p_r = \frac{a}{b + \frac{r^2}{[m^2]}} \tag{6}$$

where $a = 1.37(\pm 0.07) \times 10^{-9}$ and $b = 2.7(\pm 0.2) \times 10^{-11}$.

2.2. Data analysis

As the movement of the lid stirred the gas in the chamber we started tracking grains 0.16 s later, when the gas movement had mostly ceased and the dominating force expected to be acting on the particles was photophoresis. 120 individual

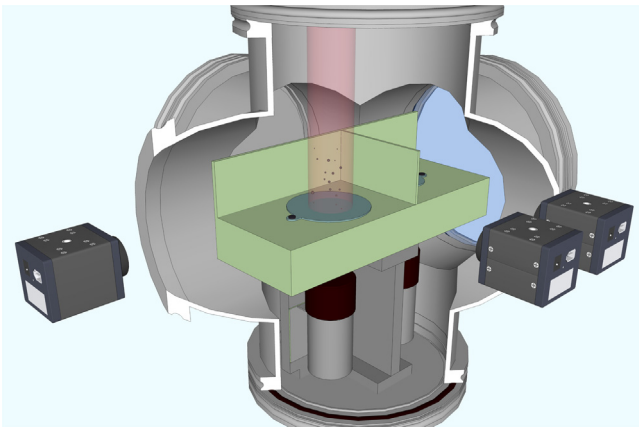

Fig. 1. Experimental setup: a dust bed with 7 cm diameter is placed in a vacuum chamber at 4 mbar ambient pressure. An infrared laser (1064 nm) with a power density of 20 kW/m^2 within a beam diameter of 3.4 cm is focussed on the basaltic dust, which is ejected. After the lid is closed the movement of airborne particles is dominated by photophoresis. Only one camera was used for the current study.

Fig. 2. Snapshot of airborne particles under microgravity.

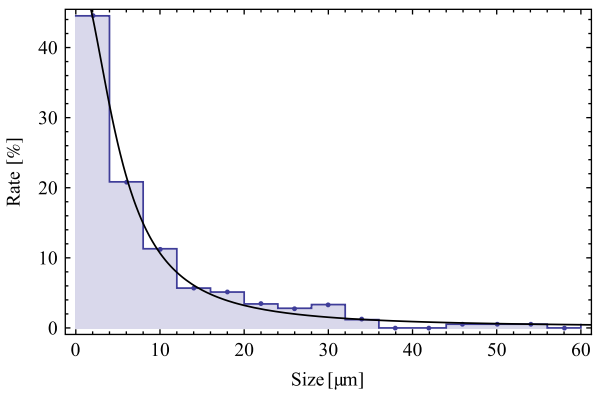

Fig. 3. Size distribution of ejected basalt (from Kelling et al., 2011b); depicted are the equivalent radii of the ejected particles. The bin width is 4 μm and the resolution limit is about 2 μm. Superimposed is a simple analytic function (see text).

particles were tracked, with trajectories classified in a small number of different types of motion, examples of which are shown in Fig. 4. The particles follow one direction on average, towards or away from the direction of illumination (see Table 1).

Superimposed on this average motion are more or less extended rotations around the average direction which in total lead to helical motions (see Fig. 4).

As $\Delta T-$photophoresis should be related to the direction of illumination, the absolute velocities in that direction are of importance. The distribution of velocities can be seen in Fig. 5. The velocity component was measured as the length of each track in the y-direction, divided by the track time. The velocity distribution should be similar to the size distribution, as for otherwise identical particles the photophoretic drift velocity scales linearly with radius (Kelling & Wurm, 2013; Wurm & Krauss, 2006). However, there is a large fraction of small particles which move in the negative direction. This can be

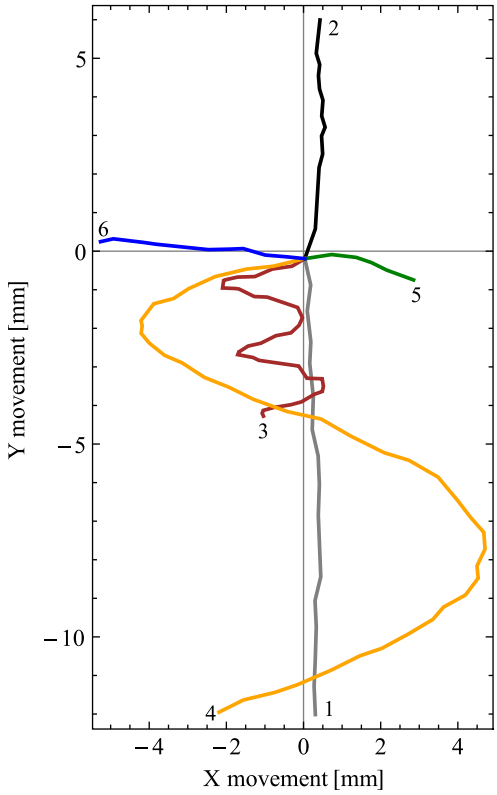

Fig. 4. A selection of the different typical particle movements, already corrected for the residual drift, (1 – grey) positive photophoresis, (2 – black) negative photophoresis, (3,4 – brown, orange) strong helical component, (5,6 – green, blue) with sideward component. (For interpretation of the references to colour in this figure legend, the reader is referred to the web version of this paper.)

Table 1
Movement characteristics of the tracked particles.

Movement	Number
Positive photophoresis (classes 1, 3, 4)	103
Negative photophoresis (class 2)	8
Perpendicular motion (classes 5, 6)	9
Total	120

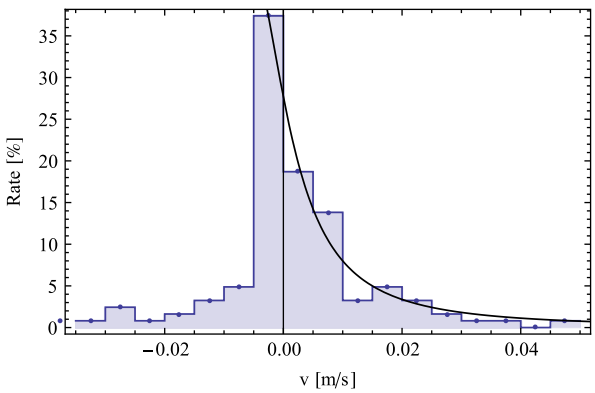

Fig. 5. Distribution of the observed particle speeds along the direction of illumination (photophoresis + gas motion); the solid line is a fit to the data (see text).

explained by a residual gas motion and an offset velocity probability has to be considered as

$$p_v = \frac{a}{b + \left(\frac{v - v_0}{c}\right)^2}. \tag{7}$$

As the values of a and b should be equal to those obtained from the dust size distribution, the scale factor between v and r is found to be $c = 1422(\pm 123)$ m/s and the offset drift velocity is $v_0 = 6.2(\pm 0.6)$ mm s^{-1}.

A rough comparison between the experimental data and the analytic solution essentially leaves only one free parameter, the thermal conductivity. The particle of mass m subject to a force F having a gas–grain coupling time τ has a terminal drift velocity of $v = \tau(F/m)$. The ratio of the terminal velocity due to the photophoretic force to the radius can be estimated as

$$\frac{v}{r} \approx \frac{33I}{v_g \lambda_p}\left[\frac{\mathrm{m}^2}{\mathrm{s}^2\mathrm{K}}\right], \tag{8}$$

where λ_p is the thermal conductivity in W/mK and I is the power density of incoming radiation in W/m^2. This estimate is based on the low pressure approximation of the photophoretic force in the free molecular flow regime

$$F_{ft_{free}} = \frac{\pi r^3 I p}{6\lambda_p T_\infty} \tag{9}$$

and the gas–grain coupling time (Blum et al., 1996)

$$\tau = \frac{0.68 m_d}{\sigma \rho_g v_g} \tag{10}$$

where σ is the dust particle cross section, ρ_g is the gas density and m_d is the mass of the dust grain. The value of v/r is given from the size and velocity distributions as the scaling factor c/[m]. At $T = 300$ K and with the molar mass of air $\mu = 28$ g/cm^3, $v_g = \sqrt{8R_gT/\pi\mu} = 480$ m/s. This leads to a value of $\lambda_p \approx 1$ W/(m K), which is on the order of the bulk value for silicates.

Earlier experiments showed that particles can decay into a large number of smaller particles after ejection from a dust bed. Particles up to mm in size were also observed, though the individual constituent grains are smaller. This implies that particles in our experiments are not just individual grains but also aggregates. For very large aggregates one might expect a strong increase in photophoresis as they might be treated by a lower thermal conductivity. However, the values of thermal conductivity estimated for these particles do not seem to support such a view.

The (new) result here is that the value of thermal conductivity is constant for all aggregate sizes as the velocity of the particles increases linearly with particle size.

In addition to the absolute strength of the photophoretic force, the experiments also allow a quantification of the direction of the photophoretic force. After correcting for the residual velocities there is still a fraction of particles moving in the negative direction. To visualize the distribution of particle trajectory directions, we determined the angular distribution of the photophoretic drift directions. As before, an average sideward drift of all tracks was subtracted to compensate for the residual gas motion. The distribution is shown in Fig. 6. About 93% of the particles fit the general idea of a positive $\Delta T-$force. A distinctive fraction of 7% shows negative photophoresis. As we could not resolve the particles spatially, we do not know what makes these particles special or what separates these groups. It could be the size, morphology or special absorption sites located within the particle.

These findings are in perfect agreement with numerical calculations of photophoretic forces, to be treated in detail in a separate publication but outlined briefly in the next section below.

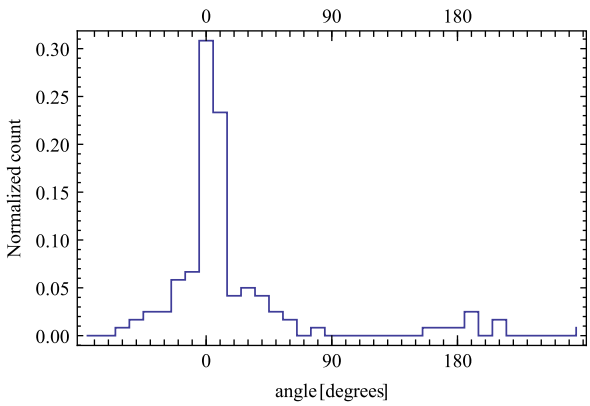

Fig. 6. Distribution of the trajectory angles with respect to the direction of illumination. 0° refers to the direction of the illumination.

3. Numerical model

A numerical model was used to compare the effect of the photophoretic force on irregular aggregates to that of spheres of the same mass. The aggregates in the model consisted of collections of spherical monomers, either of the same size (monodisperse) or of a range of sizes (polydisperse). In the model, the surface of an aggregate is defined by many patches which are used to determine the photon flux to each patch, the temperature gradient across the grain, the flux of gas molecules to the patch surface, and finally the net momentum transferred to the aggregate.

Assuming a light source along a given direction, the illumination flux is calculated at the centre of each patch taking into account the shadowing due to other monomers within the aggregate. The surface temperature was then defined by setting the average temperature of the aggregate to the mean gas temperature T, with the average temperature of a given monomer $\overline{T}_i$ determined by the fraction of its surface which is illuminated, such that shadowed monomers have a lower mean temperature than fully illuminated monomers. The temperature of each patch was then adjusted based on the illumination flux and the distance from the last illuminated point, as illustrated in Fig. 7.

3.1. Momentum transfer calculations

The incoming gas particles are assumed to move on straight-line paths which are not blocked by other monomers within the aggregate, i.e. along open lines of sight (LOS). The number of gas particles impacting a surface per unit area per unit time is given by the flux

$$I = n \iiint v \cos(\gamma) f(\boldsymbol{v})\, d\boldsymbol{v}, \tag{11}$$

where n is the particle number density, $v \cos(\gamma)$ is the component of the velocity normal to the surface, and $f(\boldsymbol{v})$ is the Maxwellian velocity distribution. The integral over the velocity may be separated into an integral over the magnitude of the velocity and an integral over the angles

$$I = n \int_0^\infty v^3 f(v)\, dv \iint \cos(\gamma)\, d\Omega. \tag{12}$$

The integral $\iint \cos(\gamma)\, d\Omega$, the LOS-factor, depends on the open lines of sight at the surface: points on an aggregate may have lines of sight which are blocked by other monomers within the aggregate, requiring the LOS-factor to be calculated numerically for each patch. Details of the method are given in Matthews et al. (2012).

Gas particles equilibrate to the local surface temperature before being re-emitted, assuming an accommodation coefficient $\alpha = 1$. Ejected particles may escape into space along an open LOS or collide with another monomer. If the rebound direction is blocked by another monomer in the aggregate, the gas is assumed to equilibrate with the new surface temperature, and the process repeats until an open rebound direction is selected. Rebounds continue until 99% of the gas has escaped; the remaining particles are assumed to rebound along the "average" open LOS for each patch.

The momentum transfer from an ejected gas particle is assumed to be cancelled if the gas particle collides with another monomer in the aggregate. Thus, the calculations consider only momentum transfer from the initial incoming gas particles and from gas particles rebounding along open paths. The magnitude of the change in momentum, and thus the force, at each patch is given by

$$F_p = \left(\frac{\Delta p_{out}}{\Delta t}\right)_p - \left(\frac{\Delta p_{in}}{\Delta t}\right)_p = mA_p\left(I'_p v_s - I_p v_g\right) \tag{13}$$

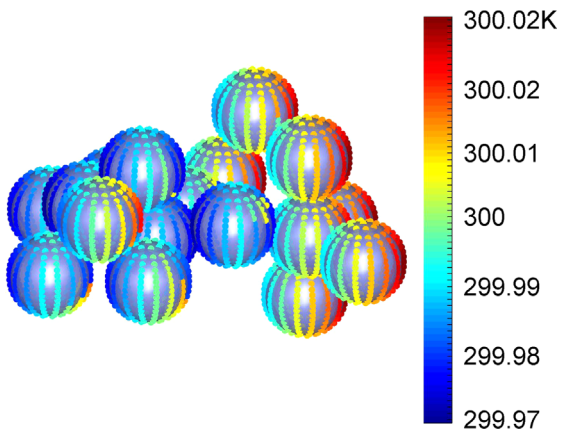

Fig. 7. Temperature gradient for an aggregate consisting of 17 monodisperse spheres, with the direction of illumination from the right. The monomers with the greatest illumination flux have the hottest temperatures.

where m is the mass of the gas particle, A_p is the area of the patch, I_p is the gas flux to patch p calculated by Eq. (12), I'_p is the flux adjusted for rebounding gas particles, v_s is the velocity determined by the surface temperature and v_g is the rms velocity of the gas. The direction of v_s is determined by the rebound direction, while the direction of v_g is along the average open LOS for a given patch. The average photophoretic force is determined by repeating the calculations numerous times and subtracting the force imparted by the gas when there is no temperature gradient present.

The components of the drift velocity of the aggregate are calculated by

$$v_{drift} = F_{ph}\tau/m_d \tag{14}$$

with τ being the gas–grain coupling time, given by Eq. (10). In this case, σ is the cross-sectional area of the aggregate projected in a plane perpendicular to the direction of the component of the force.

3.2. Numerical results

Simulations were run for two populations of aggregates, one built from monodisperse monomers ($r = 1.7$ μm) and the other built from polydisperse monomers ($0.5\ \mu m \le r \le 10\ \mu m; \langle r \rangle = 1.7\ \mu m$). The aggregates ranged in size from $N=2$ to $N=2000$ monomers, and a size distribution of the aggregates was chosen to match that given for the basalt powder shown in Fig. 3, where the radius of the an aggregate is defined by the equivalent radius, R_σ (Matthews et al., 2012). The material is assumed to be basalt with a material temperature gradient of 10^4 K/m, and the surrounding gas temperature is set to be $T=300$ K. The average force and drift velocity in the direction of illumination are normalized to that found for a single sphere with $r = 1.0$ μm ($m_0 = 1.3 \times 10^{-14}$ kg): $f_0 = 1.0 \times 10^{-14}$ N and $v_0 = 1.1$ mm/s, respectively. As shown in Fig. 8, the photophoretic force on the aggregates is similar to that acting on spheres of the same mass. The drift velocity of the aggregates tends to be smaller than that for the spheres, however, due to their open cross-sections (see Fig. 9), though the drift velocity of small aggregates, especially those consisting of monodisperse spheres, can be somewhat larger. Both types

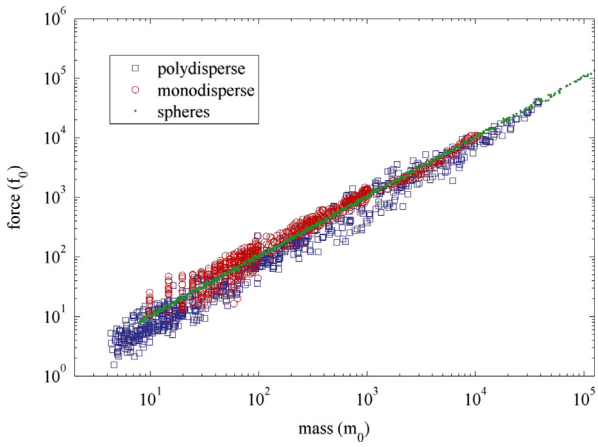

Fig. 8. Photophoretic force vs. mass, normalized to the force and mass of a sphere with $r = 1.0$ μm, $f_0 = 1.0 \times 10^{-14}$ N and $m_0 = 1.3 \times 10^{-14}$ kg.

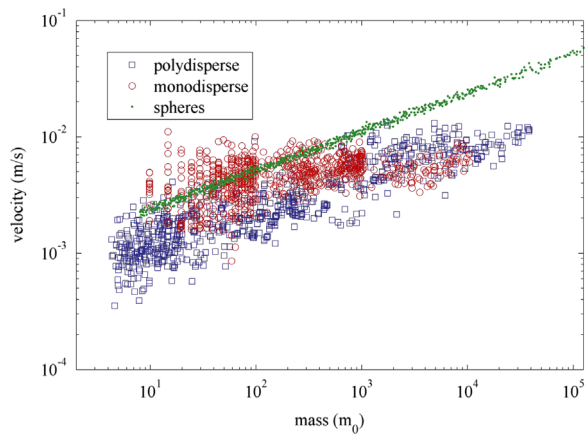

Fig. 9. Drift velocity vs. mass, normalized to the velocity and mass of a 1.0 μm−radius sphere, $v_0 = 1.1$ mm/s, $m_0 = 1.3 \times 10^{-14}$ kg. Both aggregate populations tend to have a smaller drift velocity than spheres of equivalent mass due to their larger cross-sectional areas.

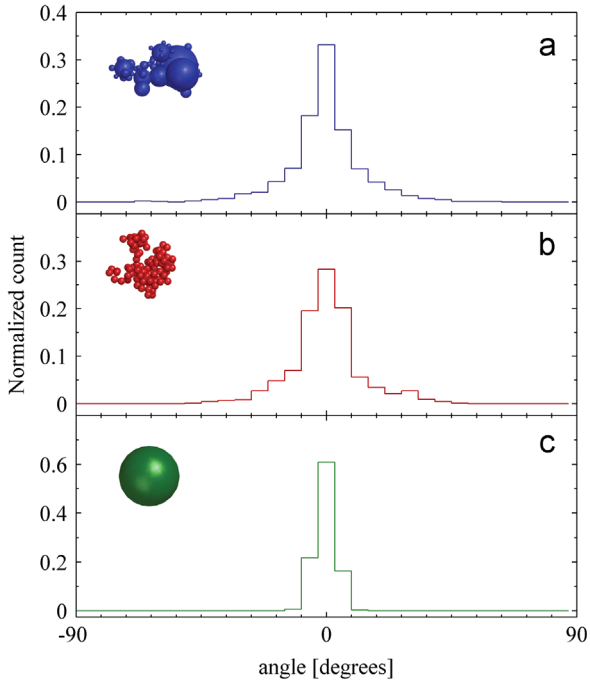

Fig. 10. Distribution in drift velocity with respect to the direction of illumination for (a) aggregates consisting of polydisperse spheres, (b) aggregates consisting of monodisperse spheres, and (c) single spheres.

of aggregates have a broad distribution of velocities about the direction of illumination (Fig. 10), whereas the distribution for the spheres is sharply peaked in the forward direction. The polydisperse aggregates, Fig. 10a, have a larger peak in the forward direction, probably due to the fact that the motion of the aggregate is dominated by the effective force on the largest monomer(s) in the aggregate, which behave more like spheres.

4. Discussion

Although the experiment and model were designed to be complementary, there are differences between the two cases. The experiments do not allow determination of the detailed morphology of the dust grains and aggregate structure, and particle sizes can only be assigned to velocities on average. The simulations, on the other hand, assume certain aggregate structures which consist of spherical monomers and assume a specified temperature gradient for an illuminated sphere. Keeping these caveats in mind, together they give the following picture.

Over the total size scale, the experimental photophoretic velocity is consistent with a linear size dependence as the probability distribution for particle size and velocity are proportional to each other. This would be expected for solid monolithic grains. Experimentally, the absolute values were fitted by adapting the thermal conductivity. Essentially all unknowns are embedded in this parameter.

The results of the simulation show the same trends. The temperature gradient over a sub-unit was fixed with illumination, which is equivalent to establishing a given thermal conductivity to each sphere. The simulations show that aggregation changes the absolute photophoretic force by a small factor of two to three at best compared to spheres of the same mass or volume, independent of the total mass. However, the drift velocity is reduced for the aggregates due to their porous structure: the mass of the aggregates scales as approximately $m \propto r^{2.5}$. This difference is reflected in slopes of the drift velocities (see Fig. 9). However, the studies also show a possible spread in the drift velocities by a factor of two to three for given mass or size.

The agreement in the absolute values of the measured drift velocities to the calculated drift velocities shows that the photophoretic forces are consistent with ΔT forces. This is also consistent with the fact that the photophoretic forces are strongly peaked in the forward direction. The deviations of several tens of degrees offset from the illumination direction are consistently seen in both experiment and simulation. Loesche et al. (2013) showed that almost spherical particles show photophoretic ΔT forces with directions deviating from the incident direction by several degrees. The basalt particles studied here are less spherical and thus have larger deviations, in agreement with this observation. As the motion of single grains (spheres) is essentially forward directed and the aggregates have a broad range of velocities (see Fig. 10), the somewhat broader peak observed in the experimental data (Fig. 6) might indicate a mix of individual grains and aggregates. Numerical and experimental data both also clearly show that sideways particle motion is possible, even in the absence of additional alignment forces.

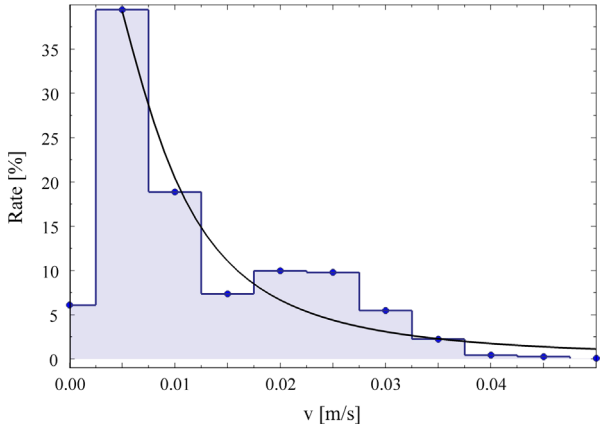

Fig. 11. Calculated distribution of particle speeds for a mix of spheres ($1 \le r \le 10$ μm) with polydisperse aggregates ($r \ge 1.5$ μm) matching the experimental results. The line is the fit that resulted from the experimental data.

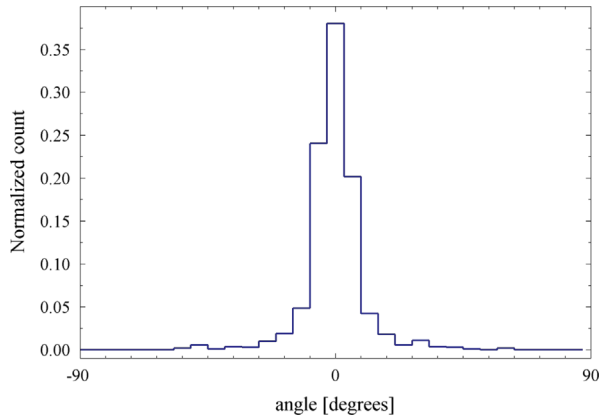

Fig. 12. Calculated distribution of velocities with respect to the direction of illumination (angles) for a mix of spheres ($1 \le r \le 10$ μm) with polydisperse aggregates ($r \ge 1.5$ μm) matching the experimental results.

Knowing the individual differences between spheres and aggregates it should be possible to match the experimental findings by a distribution of particles consisting of spheres and polydisperse aggregates. Figure 11 shows the results of a speed distribution calculated using a mix of aggregates and polydisperse spheres chosen to have a size distribution as shown in Fig. 3. The speeds are scaled by a factor 3 (accounting e.g. for the artificial temperature gradient chosen), but then match the observed experimental findings (Fig. 5) very well now as the superimposed fit from the experimental data indicates. The same mix of spheres and polydisperse aggregates also mirrors the experimental angular distribution now with the strong peak but wide wings (Fig. 12, cmp. Fig. 6).

The helical motion of particles can be understood as the particles align themselves to the illumination direction but maintain a residual torque around this direction (van Eymeren & Wurm, 2012). In this case, no net sideward motion will result in the long term as particles rotate around the direction of illumination. We note that the current measurements are related to the average observed drift directions which, due to the limited track length, can depend on the rotation frequency and initial position on a potential helix. In the case of $\Delta T-$forces we expect a continuous net sideward motion only if particles are aligned with a different direction different to the illumination. Future numerical simulations and experiments will address this behavior.

4.1. Magnetic alignment

While gravity plays no role in alignment under microgravity, magnetic fields might still act on particles with sufficient magnetization (Rohatschek & Horvath, 2010). Measurements of magnetic fields were not carried out in the experiment, though basalt can be magnetized. Values for the volume magnetization measured by eg. Cox & Doell (1962) are around $m = 4$ A/m. For a spherical 10 μm (radius) particle the total magnetization would be $M = 2 \times 10^{-14}$ A m^2. If we assume that the magnetic field within the experimental setup is on the order of the Earth's magnetic field of 50 μT, the maximum resulting torque is $D_m = 10^{-18}$ N m. This is enough to rotate magnetized particles in a few tens of ms which is short

compared to the experiment duration. Without other torques acting, we would therefore expect such particles to be aligned along the direction of the magnetic field.

In comparison, torques imposed by photophoresis on non-perfect inhomogeneous grains can be estimated as follows. The photophoretic forces measured for 10 μm grains are on the order of 10^{-11} N. If this acts on only one side of a grain, the maximum torque is $D_{Ph} = 10^{-16}$ N m, a factor of 100 larger than the magnetic torque. While this extreme is unrealistic, it is plausible that a 1% asymmetry in the alignment of the grain with the photophoretic force would be sufficient for the photophoretic torque to be comparable to the magnetic torque.

There is a difference in the motion of particles aligned along the direction of incident light or by a magnetic field pointing in a different direction. A particle self-aligned by ΔT photophoresis will afterwards only rotate around the direction of illumination. This is consistent with most of the helical motions observed in the experiment. If magnetic alignment dominates the particle motion, rotation induced by photophoresis or gas drag would be restricted to rotations around the direction of the magnetic field. This readjustment can change the magnitude and direction of the photophoretic force and might produce non-symmetric helical motions around the direction of the magnetic field. While this might be consistent with some of the sidewards trajectories, there are too few data on this to give a detailed analysis.

The direction of the Earth's magnetic field differs significantly different from the vertical, the direction of the laser light. If, however, any other remanent magnetic field within the experiment was present there is a small chance that it is aligned to the direction of illumination in which case we could not discriminate between the two types of alignment.

To conclude, we cannot rule out or confirm that particles are aligned by a remanent magnetic field within the experiment.

5. Conclusion

Micrometer-sized basalt particles entrained in a thin atmosphere will move preferentially along the direction of an illuminating light source due to ΔT forces. However, a significant fraction of a particle sample can move in directions other than the illumination direction depending on the particle orientation. To date, systematic motions in arbitrary directions not related to the illumination were often associated to $\Delta\alpha$ forces and aligning torques (gravitophotophoresis and magneto-photophoresis). This is only one possible option. We find that if particles are aligned by external forces, it is not necessarily a body fixed $\Delta\alpha$ engine; there is also a sideward movement associated with ΔT forces.

Unfortunately though, ΔT forces on basalt grains cannot be large enough to lift small basalt aggregates against Earth's gravity. The ratio between the photophoretic force at low pressure (Eq. (9)) and the gravity is

$$\frac{F_{ft_{free}}}{F_g} = \frac{Ip}{8\lambda_p T_\infty \rho_p g} \tag{15}$$

As an example, given the thermal conductivity and solar insolation on Earth (1000 W/m^2) at 2000 Pa pressure assuming a density of the particles of 3000 kg/m^3 and a temperature of $T_\infty = 250$ K, the resulting lift is only 3% of gravity. Applying photophoresis to particles in the Earth's stratosphere and mesosphere, or on the Martian surface, certain classes of particles might experience prolonged residence times (Pueschel et al., 2000), but these cannot be typical basalt particles. Either particles of lower thermal conductivity are needed or it has to be particles where $\Delta\alpha$ forces are active. The number of trajectories analyzed in our experiment was relatively small, yet there is a fraction of particles with negative photophoresis which require a more detailed analysis. Other experiments e.g. by Rohatschek (1983) on metal dust aggregates or by Kelling et al. (2011a) and van Eymeren & Wurm (2012) on micron sized ice aggregates suggest that lower thermal conductivities for certain classes of particles are feasible.

The results of this study lead to the conclusion that within the parameter range studied photophoresis on aggregates scales with their mass as for bulk particles. In this case the degree of aggregation does not change the effective thermal conductivity of a particle with respect to photophoresis.

Acknowledgements

This project is supported by DLR Space Management with funds provided by the Federal Ministry of Economics and Technology (BMWi) under Grant no. DLR 50 WM 1242, and in part by NSF Grant nos. 1002637 and 0847127. M. Kuepper is funded by the DFG. Adaptation of the experiment sketch (Fig. 1) has kindly been provided by T. Jankowski.

References

Beresnev, S.A., Kochneva, L.B., Suetin, P.E., Zakharov, V.I., & Gribanov, K.G. (2003). Photophoresis of atmospheric aerosols in the Earth's thermal radiation field. *Atmospheric and Oceanic Optics*, *16*, 431–438.

Blum, J., Wurm, G., Kempf, S., & Henning, T. (1996). The Brownian motion of dust particles in the solar nebula: an experimental approach to the problem of pre-planetary dust aggregation. *Icarus*, *124*(December), 441–451.

Cheremisin, A.A., Shnipov, I.S., Horvath, H., & Rohatschek, H. (2011). The global picture of aerosol layers formation in the stratosphere and in the mesosphere under the influence of gravito-photophoretic and magneto-photophoretic forces. *Journal of Geophysical Research (Atmospheres)*, *116* (October), 19204.

Cheremisin, A.A., Vassilyev, Y.V., & Horvath, H. (2005). Gravito-photophoresis and aerosol stratification in the atmosphere. *Journal of Aerosol Science*, *36*, 1277–1299.
Cox, A., & Doell, R.R. (1962). Magnetic properties of the basalt in hole EM 7, Mohole project. *Journal of Geophysical Research*, *67*(10), 3997–4004.
de Beule, C., Kelling, T., Wurm, G., Teiser, J., & Jankowski, T. (2013). From planetesimals to dust: Low-gravity experiments on recycling solids at the inner edges of protoplanetary disks. *Astrophysical Journal*, *763*(January), 11.
de Beule, C., Wurm, G., Kelling, T., Küpper, M., Jankowski, T., & Teiser, J. (2014). The martian soil as a planetary gas pump. *Nature Physics*, *10*, 17–20.
Haisch, C., Kykal, C., & Niessner, R. (2008). Photophoretic velocimetry for the characterization of aerosols. *Analytical Chemistry*, *80*(5), 1546–1551.
Hidy, G.M., & Brock, J.R. (1967). Photophoresis and the descent of particles into the lower stratosphere. *Journal of Geophysical Research*, *72*(January), 455.
Kelling, T., & Wurm, G. (2009). Self-sustained levitation of dust aggregate ensembles by temperature-gradient-induced overpressures. *Physical Review Letters*, *103*, 215502-1–215502-4.
Kelling, T., & Wurm, G. (2013). Accretion through the inner edges of protoplanetary disks by a giant solid state pump. *Astrophysical Journal Letters*, *774* (September), L1.
Kelling, T., Wurm, G., & Dürmann, C. (2011a). Ice particles trapped by temperature gradients at mbar pressure. *Review of Scientific Instruments*, *82*(November (11)), 115105.
Kelling, T., Wurm, G., Kocifaj, M., Klačka, J., & Reiss, D. (2011b). Dust ejection from planetary bodies by temperature gradients: Laboratory experiments. *Icarus*, *212*, 935–940.
Kocifaj, M., Klačka, J., Kelling, T., & Wurm, G. (2011). Radiative cooling within illuminated layers of dust on (pre)-planetary surfaces and its effect on dust ejection. *Icarus*, *211*(January), 832–838.
Loesche, C., Wurm, G., Teiser, J., Friedrich, J.M., & Bischoff, A. (2013). Photophoretic strength on chondrules. 1. Modeling. *Astrophysical Journal*, *778*(December (2)), 101.
Matthews, L.S., Land, V., & Hyde, T.W. (2012). Charging and coagulation of dust in protoplanetary plasma environments. *Astrophysical Journal*, *744*, 397–398.
Pueschel, R.F., Verma, S., Rohatschek, H., Ferry, G.V., Boiadjieva, N., Howard, S.D., & Strawa, A.W. (2000). Vertical transport of anthropogenic soot aerosol into the middle atmosphere. *Journal of Geophysical Research*, *105*, 3727–3736.
Rohatschek, H. (1956). Über die kräfte der reinen photophorese und der gravitophotophorese (on the forces of pure and gravito-photophoresis). *Acta Physica Austriaca*, *10*, 267–286.
Rohatschek, H. (1983). Photophoretic forces on stratospheric and mesospheric aerosols. In: *Aerosols in Science, Medicine and Technology*.
Rohatschek, H. (1995). Semi-empirical model of photophoretic forces for the entire range of pressures. *Journal of Aerosol Science*, *26*, 717–734.
Rohatschek, H. (1996). Levitation of stratospheric and mesospheric aerosols by gravito-photophoresis. *Journal of Aerosol Science*, *27*(3), 467–475 Atmospheric Aerosols.
Rohatschek, H., & Horvath, H. (2010). Magneto-photophoresis and mesospheric particles. *Journal of Geophysical Research (Atmospheres)*, *115*(December), 24208.
van Eymeren, J., & Wurm, G. (2012). The implications of particle rotation on the effect of photophoresis. *Monthly Notices of the Royal Astronomical Society*, *420*(February), 183–186.
von Borstel, I., & Blum, J. (2012). Photophoresis of dust aggregates in protoplanetary disks. *Astronomy and Astrophysics*, *548*(December), A96.
Watanabe, S.N., Iwaki, T., Kohira, M.I., Magome, N., & Yoshikawa, K. (2011). Negative photophoresis of smoke particles observed under microgravity. *Chemical Physics Letters*, *511*(August), 447–451.
Wurm, G., & Krauss, O. (2006). Concentration and sorting of chondrules and CAIs in the late Solar Nebula. *Icarus*, *180*(February), 487–495.
Wurm, G., & Krauss, O. (2008). Experiments on negative photophoresis and application to the atmosphere. *Atmospheric Environment*, *42*(11), 2682–2690.
Wurm, G., Teiser, J., Bischoff, A., Haack, H., & Roszjar, J. (2010). Experiments on the photophoretic motion of chondrules and dust aggregates: Indications for the transport of matter in protoplanetary disks. *Icarus*, *208*, 482–491.